

Article

Evaluation of the Gemological Properties of Datolites from the Campotrera Deposit in the Northern Apennines (Italy)

Luigi Marinoni ^{1,*}, Franca Caucia ¹, Mattia Gilio ¹  and Maurizio Scacchetti ² 

¹ Department of Earth and Environmental Sciences, University of Pavia, 27100 Pavia, Italy; caucia@crystal.unipv.it (F.C.); mattia.gilio@unipv.it (M.G.)

² c/o Earth Science Department, Italian Society of Mineralogy and Petrology, University of Pisa, I-56126 Pisa, Italy; mauscacchetti@alice.it

* Correspondence: luigitito.marinoni@unipv.it

Abstract: This work investigates the gemological properties of the datolite from the famous field of Campotrera near Reggio Emilia in Italy, for a possible commercial use in the market. This mineral occurs in widespread multi-centimeter veins, together with calcite and prehnite, within polygenic breccias in basaltic ophiolites. The most common form for this datolite is the double wedge with a prism (110) and a pinacoid (001). The gems obtained are mixed or carré cut, colorless or salmon pink, transparent, with a vitreous luster and weight between 1 to 5 carats. They have high brilliance, transparency and birefringence, glassy luster, absence of cleavage. The major chromophore is probably Fe, which occurs as inclusion of hematite and ilmenite. Raman investigations highlighted different fluid inclusions. The primary are randomly distributed or, in some cases, follow the growth zones, while the secondary form aligned tracks along the microcracks. Fluid inclusions can be biphasic and made up by liquid + gas (L + G), generally >10 mm in size, and more rarely, monophasic, composed only by liquid (L) generally <10 mm. The gems extracted from the rough sample are very valuable but their delicacy requires attention in the cutting and preparation of the jewels.

Keywords: Campotrera; datolite; fluid inclusions; trace elements; micro Raman spectroscopy



Citation: Marinoni, L.; Caucia, F.; Gilio, M.; Scacchetti, M. Evaluation of the Gemological Properties of Datolites from the Campotrera Deposit in the Northern Apennines (Italy). *Minerals* **2023**, *13*, 1057. <https://doi.org/10.3390/min13081057>

Academic Editor: Frederick Lin Sutherland

Received: 26 May 2023

Revised: 1 August 2023

Accepted: 4 August 2023

Published: 11 August 2023



Copyright: © 2023 by the authors. Licensee MDPI, Basel, Switzerland. This article is an open access article distributed under the terms and conditions of the Creative Commons Attribution (CC BY) license (<https://creativecommons.org/licenses/by/4.0/>).

1. Introduction

The Emilia-Romagna region has historically been important for mining and in particular, in the period between 1850 and 1910, considerable quantities of copper were extracted from open pit mines. Subsequently the mining activity decreased but resumed when the Italian Government, during the 1920s and 1930s, adopted a policy of exploitation of every resource present on the national territory; however, after the Second World War these activities were definitively suspended [1,2]. Currently, the extraction activities concerning clays for the production of ceramics, sandstone and plaster are still very important.

Nowadays researchers and mineral collectors investigate the dismissed mines of Emilia-Romagna. Furthermore, researches conducted in recent years on the ophiolites of the Apennines at Campotrera in the province of Reggio Emilia have highlighted the presence of hydrothermal veins containing the mineral datolite (Figure 1) [2,3].

Datolite is a rather rare mineral, known above all by collectors for the beauty of its crystals. This mineral was discovered in 1806 by the Danish-Norwegian geologist Jens Esmark, who gave it this name from the Greek *δατεῖσθαι*, “to divide” and *λίθος*, “stone”, in reference to the structure of the mineral. Numerous works in the last decades have been devoted to the study of the structure of datolite [4–9].

Datolite is a nesosilicate belonging to the Gadolinite group with general chemical formula $A_2Z_2XT_2O_8(O, OH)_2$ where A is occupied by Ca, Y, REE, Z by B or Be, T by Si and X by Fe^{2+} , or partially by two H atoms (to form OH⁻ groups). Hydrogen atoms can be replaced by Cl and F, Ca by Sr, Ba, Fe, Mn, Mg and K, and finally Si by Al. This mineral crystallizes in the monoclinic system (space group P21/c: a ~4.83Å, b ~7.61Å,

$c \sim 9.63 \text{ \AA}$, $\beta \sim 90.15^\circ$) and generally occurs in the form of typically short and prismatic crystals, transparent or translucent with a color ranging from white, greyish, pale green, yellow, pink and red. It frequently shows a glassy luster, rarely resinous, and conchoidal or irregular fracture. Faceted gems have high brilliance but little fire or dispersion, while massive, brown or white colored datolites can be cut into cabochons. Due to these beautiful characteristics, datolite has also been proposed as a precious cut stone, although its low hardness (about 5 on the Mohs scale) makes it very vulnerable to abrasion and scratches and, consequently, it quickly alters [10,11].

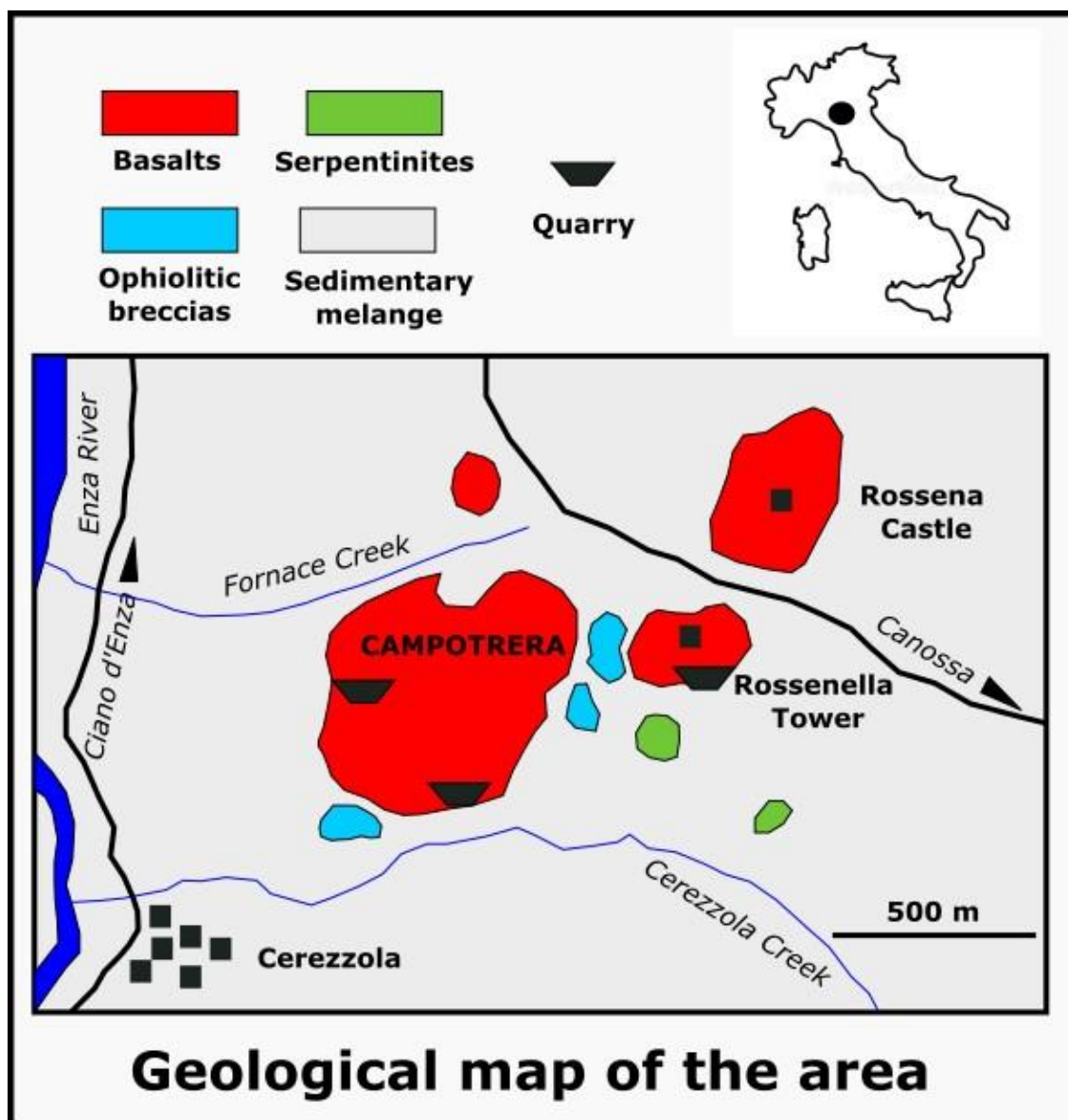


Figure 1. Geological map of the Campotrera area in the Northern Apennines. The black circle represents the location in Italy of the Campotrera field region while the rectangular symbols represent the outcropping lithologies. The black line with the arrow indicates the route towards the town of Canossa.

In addition to these aesthetic uses, datolite is also important as an industrial mineral especially in the production of special ceramics in the electrical sector [12,13]. Datolite commonly occurs in cavities and veins, especially in basalts and gabbros and is generally considered a low temperature mineral formed by hydrothermal, diagenetic or low-grade

metamorphic processes. More rarely, it is associated with other lithologies like serpentinite, limestone, hornblende, schists, granite, gneiss and skarn [2,3,14–18].

Datolite crystals of considerable value are present in numerous localities in Europe, in particular in Norway near Arendal and north of Hardangerfjord, in Austria in South Tirol, in Bosnia-Herzegovina in the province of Konjic and in Germany at St. Andreasberg in the Harz Mountains [10,11,19]. In other areas of the world, there are beautiful green, yellow and transparent crystals in Russia at Dalnegorsk in the Primorskiy Kray [18], light apple green, blue green, green yellow crystals at Roncari quarry near East Granby in Connecticut and in the Lane quarry near Westfield in Massachusetts. There are large euhedral and transparent crystals of datolite, associated with veins of calcite, in Rhode Island, while porcelain-like pink and white datolite masses occur in the Cu deposits of Lake Superior, between the United States and Canada. Beautiful datolite crystals are also found in the Copper mine of Iwato in Japan and in Charcas, San Luis Potosi in Mexico [10,11,19]. Besides the Northern Apennines, other Italian localities with datolites are Pitigliano and Impruneta in Tuscany [5] Alpe di Siusi in Trentino-Alto Adige [20], Baveno in Piedmont [21] and Valleggrande in Liguria [22].

This work mainly focuses on the petrographic, physical, gemological and chemical properties of the Campotrera datolite crystals, to determine their value for a possible use in handicrafts and jewelry. We also tried to determine the causes for the color, the chromophore elements and the types of inclusions present. Accurate investigations on the petrological processes that have formed these datolites are presented in other works [3].

2. Geological Setting of Campotrera

The area with the datolite outcrop is included within the “Riserva Naturale Rupe di Campotrera”, which extends for about 42 hectares in the Municipality of Canossa, in the Province of Reggio Emilia. The reserve was established to protect and enhance the numerous and relevant natural and artistic aspects of this area [23]. Datolites occur extensively within hydrothermal veins in an outcrop of volcanic rocks, located around a quarry (Figure 1) [1,2,14,23,24].

The ophiolites of the Northern Apennines represent portions of the oceanic lithosphere of the ancient Piedmont-Liguria Basin and of the overlying pelagic sedimentary cover; they consist of serpentinitized peridotites, spilitic basalts, ophiolitic breccias, “hydrothermalites” and rare gabbroic metasomatic rocks. In some cases, these ophiolites are associated with continental crustal rocks such as granites and granulites, suggesting that they formed in an ocean-continent transition zone, similar to modern non-volcanic continental margins [23–29] (Figure 1).

The basalts of the Campotrera-Rossena area belong to the External Liguride, represent the major ophiolitic outcrops in the province of Reggio Emilia and consist of augitic clinopyroxene, plagioclase and, subordinately, olivine, ilmenite and traces of various oxides. They are extensively metasomatized and have a high sodium content [26]. These basalts appear as massive or pillow and are defined spilitic: their original igneous paragenesis was replaced by another of low metamorphic grade, in zeolite and/or green schist facies, following metasomatic processes linked to ocean floor metamorphism. The interaction between seawater and basaltic rock during hydrothermal processes causes the release of SiO_2 and the mobilization of Ca, which can lead to the crystallization along the fractures of minerals such as calcite, datolite, quartz, prehnite and pumpellyite (Figure 2).



(a)



(b)

Figure 2. (a) Pillow-lava section (\varnothing 60 cm) within an ophiolitic breccia at Campotrera; (b) reddish vein of datolite at Campotrera (200 cm long \times 7 cm thick).

The mineralogist Franco Anelli discovered the presence of datolite in the spilitic basalts of Campotrera in 1922 (Figures 3–6). Generally, the dimensions of the crystals do not exceed one cm. However when the mining activity was intense, druses with crystals up to 5 cm were frequently found [2,30]. Authors such as Bertolani [30], Ferrari [31] and Maddalena [32] recognized as many as 54 different forms of datolite in the Rossena deposit, 16 of which were new; the more frequent habitus was defined by Bertolani as “double wedge”, where the prism (110) and the pinacoid (001) prevail (Figures 4 and 5).



Figure 3. Datolite crystal from the Campotrera field; the crystal is 1.7 mm long. Photo by Enrico Bonacina.

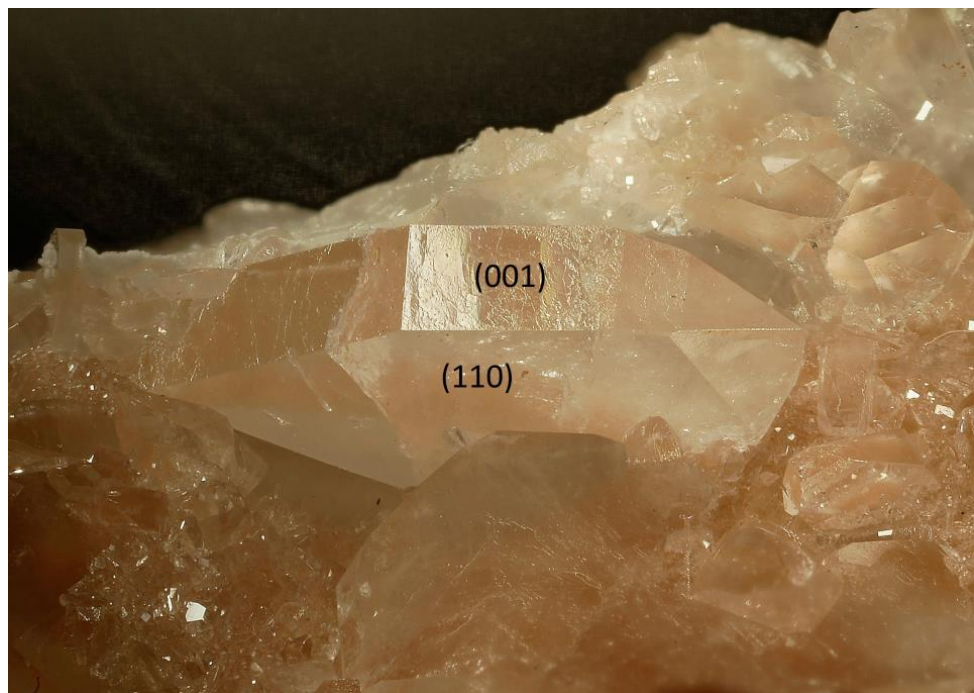


Figure 4. Light pink datolite from the Rossena-Campotrera field, 6 mm long. The crystal is double wedge with a prism (110) and a pinacoid (001). Photo by Enrico Bonacina.

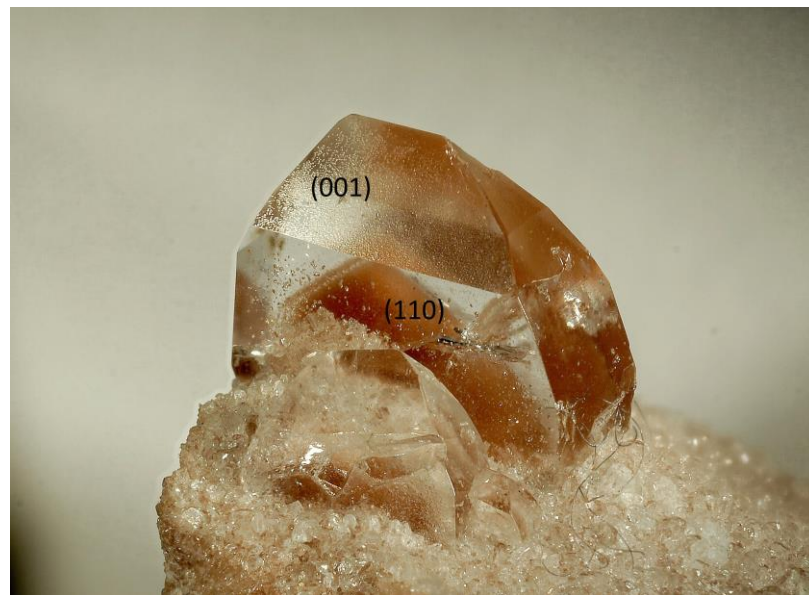


Figure 5. Reddish-pink datolite crystal from the Campotrera field, about 4 mm long. The crystal is double wedge with a prisme (110) and a pinacoid (001). Photo by Enrico Bonacina.



Figure 6. An unusual crystal (4.3 mm) of datolite from the Campotrera field. Photo by Enrico Bonacina.

A second habitus, described by Bertolani [2,30], consists of a flattened crystal according to the pinacoid (001). Characteristic of this locality, although quite rare, are the pink or deep red datolite crystals, highly sought after by collectors (Figures 4 and 5).

In the basalts of Campotrera-Rossena, there is also prehnite (Figure 7), a typical mineral deriving from metasomatic processes on the basalts of the ocean floors, and subordinately pumpellyite, in light green acicular crystals, while feldspathoids and zeolites are less frequent. Ref. [3] investigated the formation processes of the datolites that crop out in various localities of the Northern Apennines, including Campotrera.



Figure 7. Greenish-white prehnite crystals from the Campotrera field, about 7.5 mm. Photo by Enrico Bonacina.

Based on petrographic and geochemical investigations and on the salinity present in the fluid inclusions, these authors believe that these datolites are not of magmatic or hydrothermal origin, but rather diagenetic [3].

3. Materials and Methods

Most of samples investigated in this work come from old collections of various collectors in the area while others were collected by the authors at the Campotrera outcrop. We performed standard gemological analyses on twelve gems cut from rough samples, to describe optical properties, specific gravity, and ultraviolet fluorescence. Density was measured using a Presidium PCS100 Sensible Hydrostatic Balance (Presidium Instruments Pte Ltd., Singapore, Singapore). Most of the gems analysed in this study are transparent and colorless, therefore it was not necessary to use a colorimeter, while for the few that have a pinkish color we used the RGB (red, green, blue) table color system. We measured the refractive index with the distant vision method using a Kruss ER6040 refractometer (A. Kruss Optronic, Hamburg, Germany) in the 1.45–1.80 range, and a contact liquid with a RI of 1.80. Ultraviolet fluorescence was investigated with a shortwave (254 nm) and long-wave (365 nm) UV lamp (Power 3W, 20 cm distance of observation). We prepared thin section on three samples of bulk rock to carry out microscope observation. We carried out X-ray powder analyses (XRPD) to determine the mineralogical composition of two samples of bulk rock, using a Philips PW1800 Powder Diffractometer (Philips, Eindhoven, The Netherlands), with CuK α radiation ($\lambda = 1.5418 \text{ \AA}$) and a scan speed of $1^\circ/\text{min}$, in the $2\text{--}65^\circ 2\theta$ range. The samples for the analyses (about 3 g) were previously ground in an agate mortar and reduced to a very fine powder (about 5 microns). Qualitative and semi-quantitative evaluation was performed with X'Pert HighScore 5.1 (Malvern Panalytical Ltd., Malvern, UK), which is designed to obtain all phase information from loose and pressed powders and other polycrystalline samples [33].

Major element analysis (Si, Mn, Ca, Fe) was carried out on some selected crystals with a TESCAN Mira XMU Electron Microscope (Tescan Orsay Holding, Brno-Kohoutovice, Czech Republic) coupled with an EDAX system with energy dispersion and no internal standard (analytical error of about 3%). The accelerating voltage was 20 KV, while the area of the analysis was $100 \times 100 \mu^2$. The accuracy of the analyses is related to the calibration of the detector and the maintaining of standard conditions during the work. We measured the Raman spectra of fluid inclusions in datolites with a Horiba LabRam HR Evolution spectrometer (grating of 2400 groove/mm, Horiba France SAS, Longjumeau, France), equipped

with an Olympus BX41 microscope (Olympus Italia S.R.L., Segrate, Italy). We conducted the analyses on the inclusions previously observed under the microscope. Raman spectra were collected in the spectral range 100–4000 cm^{-1} averaging three accumulations of 10 s scans. The wavelength of the laser is 532 nm while the power is 10 mW.

4. Results

4.1. Gemological Analyses

From the rough samples of datolites we extracted numerous gems, which allowed us to evaluate the gemological properties of the mineral. We cut the gems following with various styles, in particular carré, baguette and mixed and different shapes like oval, pear, trapezoid, square, triangle, rectangular. The gems have small dimensions not exceeding one centimeter and their carat weight varies between 0.9 and 5.04 carats (Figure 8).

Table 1. Gemological properties of datolite from Campotrera. * RGB Color System salmon4: # FA8072 (R250 G128 B114) Standard deviation values are the following: RI: 0.004, Weight: 0.01, Specific gravity: 0.02.

Sample	Cut	Shape	Color (RGB)	Reflection Index	Weight (ct)	Specific Gravity
1	Brilliant modified	Trapezoidal	Colorless	$x = 1.62; y = 1.65; z = 1.67$	3.12	3
2a	Brilliant modified	Oval	Colorless	$x = 1.62; y = 1.65; z = 1.67$	3.41	2.99
2b	Brilliant modified	Rectangular	Colorless	$x = 1.62; y = 1.65; z = 1.67$	4.77	2.99
2c	Brilliant modified	Square	Colorless	$x = 1.62; y = 1.65; z = 1.67$	3.09	2.99
2d	Baguette	Rectangular	Colorless	$x = 1.63; y = 1.65; z = 1.67$	0.91	3
3	Brilliant modified	Pear	Colorless	$x = 1.63; y = 1.64; z = 1.67$	5.04	3
4a	Brilliant modified	Pear	Colorless	$x = 1.62; y = 1.65; z = 1.67$	3.04	3
4b	Brilliant modified	Oval	Colorless	$x = 1.62; y = 1.66; z = 1.67$	1.35	2.98
4c	Carré	Square	Colorless	$x = 1.62; y = 1.65; z = 1.67$	2.68	2.98
5d	Brilliant modified	Oval	Colorless, salmon4 *	$x = 1.63; y = 1.64; z = 1.67$	2.25	2.99
5e	Brilliant modified	Rectangular	White, light salmon4	$x = 1.62; y = 1.65; z = 1.67$	2.22	3

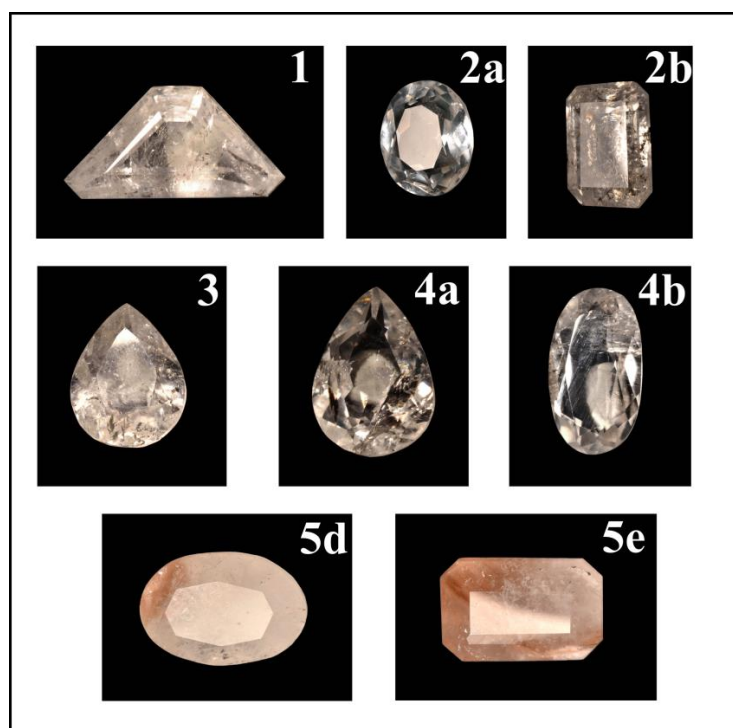


Figure 8. Gems extracted from the datolite samples from Campotrera. The gemological properties of the gems in the photos are reported in Table 1. Photo by Enrico Borghi.

The gems are transparent and colorless, with the exception of specimens 5b–e, which have a pinkish color and are translucent. Overall, gemological analyses conducted on 11 gem-quality crystals (1, 2a, 2b, 2c, 2d, 3, 4a, 4b, 4c, 5d, 5e) yielded similar results (Table 1).

Specific gravity (density) is around 3, while refractive index values vary between 1.62 and 1.67: these values are in the range of those in literature [10]. The maximum value of birefringence, calculated on the refraction indices, resulted of 0.045. Observations under the gemological microscope show, in many crystals, the presence of fractures and polyphasic inclusions, which can be biphasic, brilliant fluids, brown crystalline, polygonal, irregular, kidney-shaped, elongated tubular, discoidal, punctiform.

4.2. Petrographic Observations

The datolite-bearing basalt is strongly altered, almost completely oxidized with a weakly porphyritic and intersertal structure. We can observe pseudomorphic olivine immersed in microcrystalline matrix consisting of albite in squat or elongated twin crystals with arborescent appearance, chlorite and granules of opaque minerals like hematite and perhaps ilmenite. We also observe several relict pyroxenes, recognizable by the double cleavage marks at 90°. The plagioclase crystals are almost entirely transformed into albite (as observed from the Electron Microprobe chemical data); this transformation is typical in rocks that underwent extensive oceanic hydrothermal alteration. Overall, the microscopic observations on the basalts highlighted the strong alteration caused by the circulation of the ocean hydrothermal fluids. Subsequently, the tectonism formed the numerous polygenic breccias, also with palombine-type sedimentary clasts, which are frequent in the Campotrera ophiolite. Instead, the datolite crystals are large, fresh, without alterations or traces of cleavage and host many fluid and mineral inclusions. They also show different interference color orders (up to the fourth order) that, together with the different grain size, allow them to be distinguished from calcite (Figure 9).

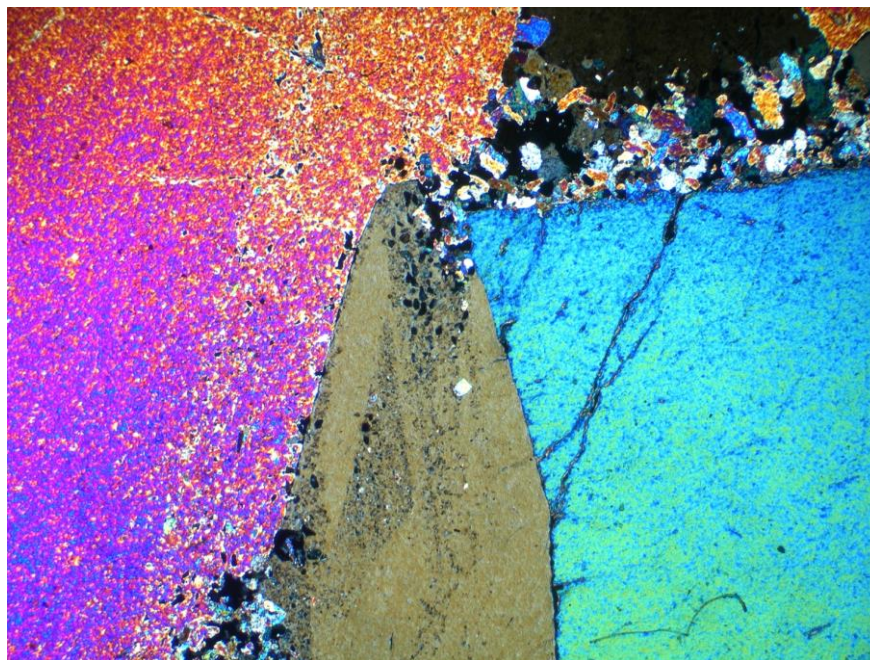


Figure 9. Thin section (crossed nicols observation) of the Campotrera datolite crystals (big and small), showing the triple junction and hematite opaque inclusions. Photo by Omar Bartoli.

The datolite crystals show a very particular texture: we can observe large crystals with triple point junction and smaller crystals at the contact with the encasing rock, with a preferential orientation along the seams. The datolite crystals also match perfectly with the salbands of the calcite veins. Datolites also have many inclusions of dark opaque crystals of hematite, partly with polygonal habitus, parallel to the growth faces, with swarms of small

calcite, crystals. Some transparent crystals show areas delimited by different interference color, with the same shape of the external surface, which create the illusion of “ghost” crystals. These morphologies might be due to compositional variations of the hydrothermal solution during crystal growth.

4.3. XRPD Analyses

We conducted X-ray Powder Diffraction Analyses (XRPD) on two samples of bulk rock to evaluate their mineralogical composition; the XRD patterns and the results of the semi-quantitative evaluation are reported in Figures 10 and 11. The XRPD analyses confirmed the presence of datolite, with contents around 30%. Others mineral the make up the rocks are albite, chlorite, mixed-layer (corrensite) and pumpellyite. This mineralogical composition appears to be consistent with the nature of the rocks, composed of altered basalts.

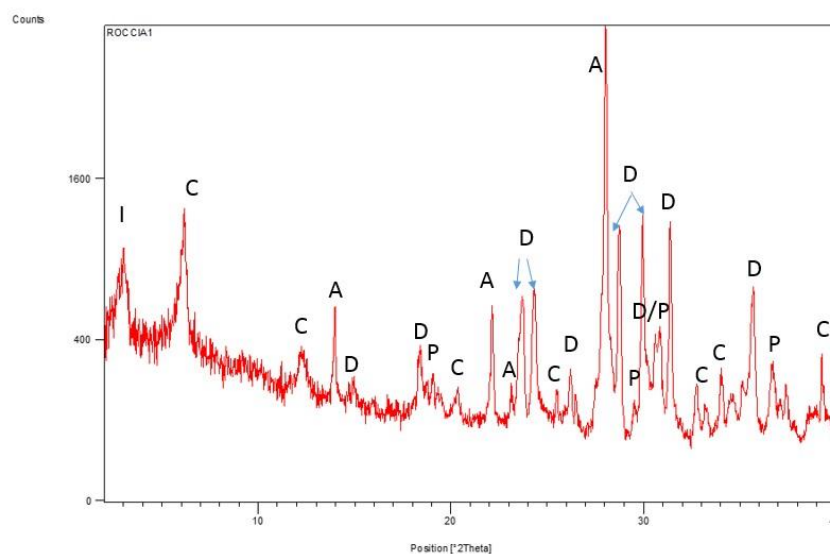


Figure 10. X-ray powder diffractogram of sample 1. Legend: D = datolite, A = albite, P = pumpellyite, C = chlorite, I = mixed-layer. Semi-quantitative analysis (%): datolite 35, albite 30, pumpellyite 15, chlorite 10, corrensite 10.

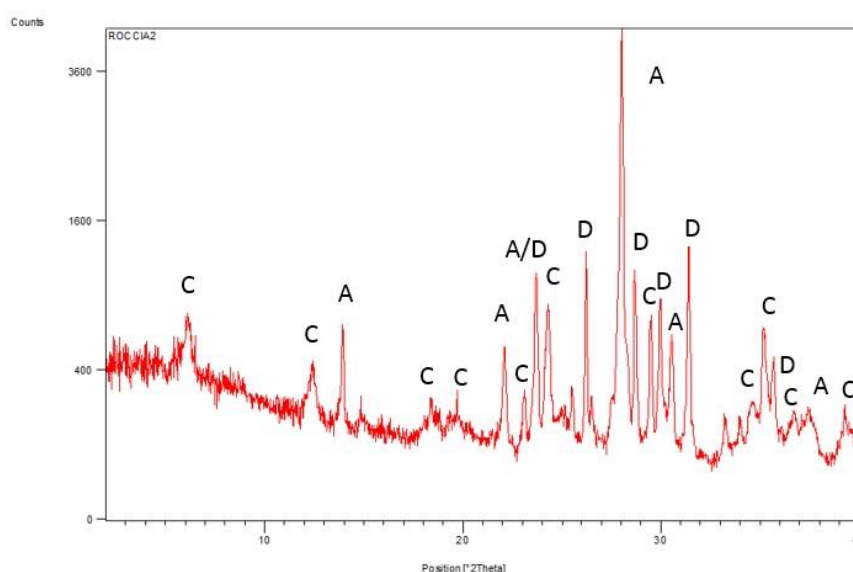


Figure 11. X-ray powder diffractogram of sample 2. Legend D = datolite, A = albite, C = chlorite. Semi-quantitative analyses (%): datolite 30, albite 60, chlorite 10.

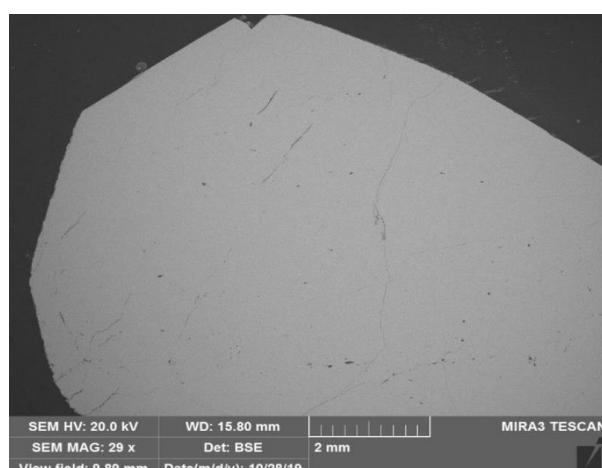
4.4. EDS and SEM Analyses

We carried out Electron Microprobe investigation on two samples of datolites (samples 3 and 5) to determine their major element composition and chemical formulas. Values are expressed as oxides (wt %) and have been recalculated as atoms per unit formula (a.p.f.u; Table 2). The formulas were calculated for 5 anions ($4\text{O}^{2-} + \text{OH}^-$).

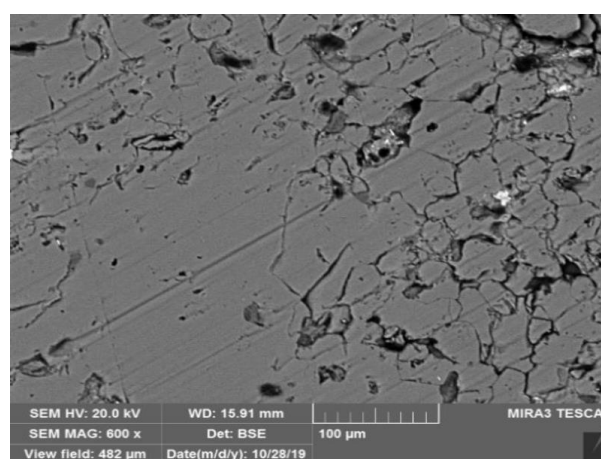
Table 2. Major elements composition of two samples of datolites obtained by SEM. The content of B_2O_3 and H_2O were stoichiometrically imposed [18].

Wt%	Datolite 3	Datolite 5A
SiO_2	37.938	38.362
CaO	34.615	34.035
Fe_2O_3	0.000	0.080
$\text{B}_2\text{O}_{3\text{calc}}$	21.802	21.865
$\text{H}_2\text{O}_{\text{calc}}$	5.645	5.658
TOT	100.000	100.000
a.p.f.u. per 5 anions ($4\text{O}^{2-} + \text{OH}^-$)		
Si^{4+}	1.008	1.016
Ca^{2+}	0.985	0.966
Fe^{3+}	0.000	0.002
B^{3+}	1.00	1.000
OH^-	1.000	1.000
TOT	3.993	3.984

SEM analyses confirmed that the mineral investigated is indeed a datolite, as the main elements identified are Si, Ca and B, which are the constituents of this mineral. We also acquired some backscattered electron (BSE) images, which allow investigating the morphology of the mineral: in particular, we can observe the homogeneous, fresh and non-flaking appearance of datolite of sample 3 (Figure 12a) while in the sample 5 we observe albite, titanite, and spongy datolite (Figure 12b).



(a)



(b)

Figure 12. Backscattered electron images of samples 3 (a) and 5a (b); in (a) we observe a crystal of datolite while in (b) we observe albite (darker areas) and titanite (lighter areas).

4.5. LA-ICP-MS Analyses

We carried out LA-ICP-MS analyses on two datolite samples (samples 3 and 5a) to determine the trace element abundances. On the sample 3, we analysed five different points; in this case trace elements are very low and do not show significant variations

(Table 3). The only element detected in relevant amount is Fe, with contents between 20 and 58 ppm. We also detected Sr and V but with negligible contents, around 1 ppm.

Table 3. Minor and trace elements composition of the sample 3 obtained by LA-ICP-MS.

Element (ppm)	SPOT 1	SPOT 2	SPOT 3	SPOT 4	SPOT 5
Sc	0.98	0.921	0.936	0.838	0.746
Ti	0.6	0.59	0.82	0.45	0.7
V	1.027	0.986	0.973	1.018	1.065
Mn	0.76	0.7	0.53	0.36	0.71
Fe	19.87	41.54	34.56	57.81	25.64
Co	0.0145	0.0195	0.0186	0.0155	0.0116
Ni	0.176	0.222	0.126	0.192	0.156
La	0.0157	0.0058	0.061	0.105	0.559
Sr	1.653	1.514	1.482	1.637	1.529
Rb	0.0212	0.0184	0.0217	0.0160	0.0182
Cs	0.0158	0.0103	0.0106	0.0199	0.0127
Ba	0.036	0.00	0.00	0.0027	0.0086
Cu	0.58	0.082	0.087	0.093	0.104
Zn	0.48	0.34	0.42	0.5	0.23

In sample 5a, we analysed 12 points from the white to the pink areas to evaluate whether the chromatic variations are due to the compositional ones (Table 4, Figure 13). The points with white color are the 1, 2, 10, 11 and 12 in Table 4. The analyses on sample 5a showed several trace elements in variable amount, in particular Fe is the most abundant with contents between 34 and 1437 ppm, followed by lower Sr (5.5–42 ppm), Ti (1–54 ppm), V (1.2–77 ppm), and Mn (1–19 ppm). Other elements, like Sc (0.6–9 ppm), Cu (up to 7.5 ppm), Zn (up to 8 ppm) are low or also below detection limits [34].

Table 4. Minor and trace elements composition of the sample 5a obtained by LA-ICP-MS.

Elem. (ppm)	SPOT 1 *	SPOT 2	SPOT 3 *	SPOT 4 *	SPOT 5	SPOT 6	SPOT 7 *	SPOT 8	SPOT 9 *	SPOT 10	SPOT 11	SPOT 12
Sc	0.49	0.71	0.64	0.89	0.68	0.77	0.92	0.59	0.91	0.70	3.21	9.28
Ti	0.44	3.35	3.92	3.61	6.62	19.49	53.24	1.09	11.71	2.15	0.89	0.97
V	1.36	1.30	1.49	1.69	1.27	1.85	4.79	1.26	7.11	1.26	1.20	1.4
Mn	2.14	3.35	2.08	7.54	3.52	3.47	18.94	0.94	2.11	1.63	2.04	3.47
Fe	27.79	69.86	133.58	313.68	131.81	135.38	1070.8	23.3	1437.4	57.92	18.04	34.64
Co	0.02	0.07	0.07	0.25	0.10	0.08	0.56	0.02	0.07	0.03	0.02	0.03
Ni	0.19	0.43	0.29	0.83	0.87	0.25	1.35	0.09	0.27	0.18	0.20	0.24
La	0.34	0.65	0.62	3.75	3.19	0.52	0.69	0.44	0.61	0.82	1.81	1.6
Ce	0.10	0.24	0.57	1.86	2.54	0.57	0.93	0.90	1.19	2.15	5.39	5.69
Sr	21.05	13.13	11.07	25.49	7.75	5.54	6.36	5.54	5.64	5.67	19.58	41.88
Rb	0.02	0.04	0.02	0.07	0.07	0.09	0.60	0.01	0.08	0.02	0.02	0.02
Cs	0.02	0.02	0.02	0.02	0.02	0.02	0.05	0.01	0.02	0.02	0.01	0.02
Ba	0.07	0.01	0.05	0.09	0.05	0.11	0.48	0.01	0.17	0.04	0.02	0.01
Cu	0.41	0.08	0.07	0.09	0.09	0.11	0.12	0.08	0.10	0.09	7.65	0.09
Zn	0.71	0.29	0.36	0.55	0.49	0.49	1.85	0.57	1.63	0.74	7.75	0.26

* Spots marked in Figure 13.

Overall, we observe that the element that increases most significantly from the white to the pink areas is Fe, which passes from about 40 ppm to 550 ppm. Ti also increases albeit less significantly, from 1.5 to 18 ppm. Mn and V are very low but increase slightly, passing from values of 2.5 and 1.3 ppm to of 5.8 and 3.3 respectively. We can therefore deduce that in the Campotrera datolites the Fe is the main chromophore element responsible for the color, followed to a much lesser extent by Ti and Mn. LAM analyses also showed that Fe is mainly concentrated in the microinclusions, made up of Fe oxides/hydroxides. Sr shows an inverse trend and decreases from the white to the pink areas, passing from about 20 ppm to 5 ppm; Sr could act as a lithophile element and replace Ca in the structure, but it is not a chromophore (Table 4). The work [3] reports some analyses of trace elements

on one sample of datolite from Campotrera but chromophores such as Fe and Mn are not reported. Compared to this work we found higher quantities of Ti and V and lower La.

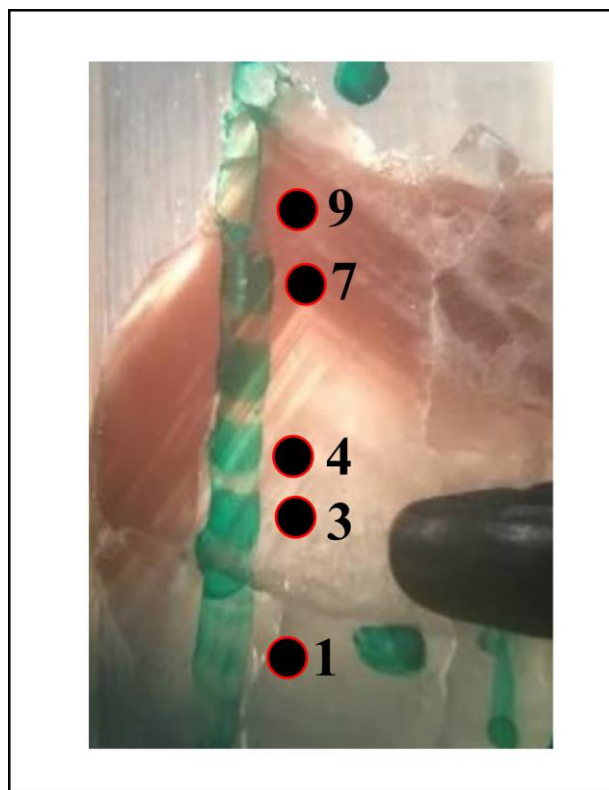


Figure 13. Section of the sample 5a (70 micron). The black dots show the polychromy and their chemical composition is reported in Table 4.

4.6. Raman Spectroscopy Analyses

The study of inclusions is very important not only in petrology but also in gemology, as it is used to identify the type of gem, its geographical origin, whether synthetic or natural and any treatment it has undergone. The latter points are especially relevant for other gems, as synthetic or treated datolites are not used in jewelry. Furthermore, inclusions can cause some valuable optical phenomena such as asterism and chatoyancy, and are considered for clarity classification. Lastly, if too abundant, inclusion may affect the transparency of the host mineral. The Raman analyses on the inclusions in the datolites under study have highlighted important compositional variations, which can be referred to different geological processes [35]. In particular, we observed aqueous inclusions with gaseous methane (biphase L + G), aqueous (L) and methane inclusions; these different typologies would indicate a reducing environment during crystallization by a carbon-rich fluid [34]. The spectrum of water, when coordinated with cations, changes in the O–H stretching region.

The Raman bands of water consist of two major modes of O–H stretching at 3657 and 3756 cm^{-1} , plus a weak O–H bond folding band at 1595 cm^{-1} . In addition, we observe strong overlapping bands in the O–H stretching region from 2750 to 3900 cm^{-1} and a weak folding band at about 1630 cm^{-1} . This spectral complexity derives from the strong interactions between the water molecules, due to the O–H–O bridging intermolecular bonds.

An important application of Raman spectroscopy is the identification of the gases present in fluid inclusions, as many gases have only one strong symmetrical stretching band. As the fluid density (P) increases, a progressive shift towards a lower wavenumber is observed. Raman analyzes make it possible to identify the presence of CO_2 , CH_4 , N_2 , and also hydrocarbons heavier than CH_4 . The Raman spectrum of CO_2 has two strong bands at 1285 and 1388 cm^{-1} and two weak symmetrical ones below 1285 cm^{-1} and

above 1388 cm^{-1} (Fermi bands). The fluid inclusions analyzed have variable dimensions, between 5 and $50\text{ }\mu\text{m}$ and exceptionally up to 0.1 mm , and spherical, elongated, hammered or irregular morphological shapes. On the other hand, we did not observe inclusions of a regular polygonal shape, sometimes present in other cases.

In general, fluid inclusions can be classified into two types: primary inclusions, which form and remain trapped during the growth of the host crystal, and secondary, which develop after crystal formation, through the filling of the fractures [35–38].

In our datolite crystals, the primary fluid inclusions are randomly distributed or, in some cases, follow the growth zones, while the secondary form aligned tracks along the microcracks. Based on the number of phases at ambient temperature, the fluid inclusions we found are as follows: (1) liquid + vapor (L + G) biphasic inclusions, generally $>10\text{ }\mu\text{m}$ in size, where the vapor bubbles occupy less than 20% of the volume; (2) more rarely, monophasic liquid inclusions (L) generally $<10\text{ }\mu\text{m}$.

We performed preliminary analyses to estimate the Na-equivalent salinity of fluid inclusions in datolites from their Raman spectrum using the semi-quantitative method by [39]. This method allows for quick estimates of the salinity of fluid inclusions from the skewing parameters of the Raman spectra in the OH-stretching region ($2800\text{--}3800\text{ cm}^{-1}$) with a relative error of about 15% [35,38]. In Tables 5 and 6 we report the salinity values of fluids in the inclusions of our samples and in those from different geological settings reported in literature [3,37].

Table 5. Salinity values of the fluids in the inclusions of Campotrera datolite, compared with those from different geological context (modified from [3,15]).

Sample 3-Fluid Inclusion	Salinity (%)
01	3.74 ± 0.57
03	3.16 ± 0.48
04	3.64 ± 0.55
06	3.37 ± 0.51
Salinity (%) Campotrera [3]	Salinity (%) Hungary [15]
10–16	1.8–2

Table 6. Salinity values of the fluids of different geological contexts [3,37].

Geological Setting	Salinity
Diagenetic fluids	9%–25%
Magmatic exhalative fluids	2%–10%
Seafloor hydrothermal fluids	3.50%–10%
Seawater evaporated with gypsum saturation	10.50%–11.50%
Magmatic fluids	28.5%–30%
Fluids in veins of quartz and calcite in sulfide mineralizations in the Northern Apennines basalts (Italy)	1.5%–4%
Recycled seawater	3.5%
Seawater	3.2%
Freshwater	0.5

The measured values of salinity (Table 6) appear rather homogeneous and around 3%–4% considering the uncertainty of the method. Previous chemical and microthermometric analyses of fluid inclusions in datolites from various ophiolitic localities in the Northern Apennines suggested that the crystal formed at a temperature of around $200\text{ }^{\circ}\text{C}$ from a fluid with a salinity of around 10%–16% NaCleq [3]. The low salinity values measured point out to a genesis of the datolite crystals other than ocean floor metasomatism, as occurred for epidote and prehnite, and was probably sedimentary. The salinity values detected by [3] are much higher than ours: however, these authors present only one analysis, while in our work we measured the salinity of four fluid inclusions.

In the work [16], fluid inclusions of datolites belonging to a geological context similar to that of Campotrera are analyzed and the salinity values appear closer to ours (Table 5). Nonetheless, we believe that the origin of the Campotrera datolites still appears uncertain and it is necessary to perform further investigations to clarify it.

Below we report the description of some fluid inclusions (I) of sample 3; the Raman graphics are reported in Appendix A, Figures A1–A10.

I1: Probably primary aqueous inclusion (P); the Raman band of H_2O is at about 3250 cm^{-1} . In the lower part of the inclusion, we observe a bubble of gaseous CO_2 ; the weak absorption band of CO_2 can be observed at about 1400 cm^{-1} (Figure 14).

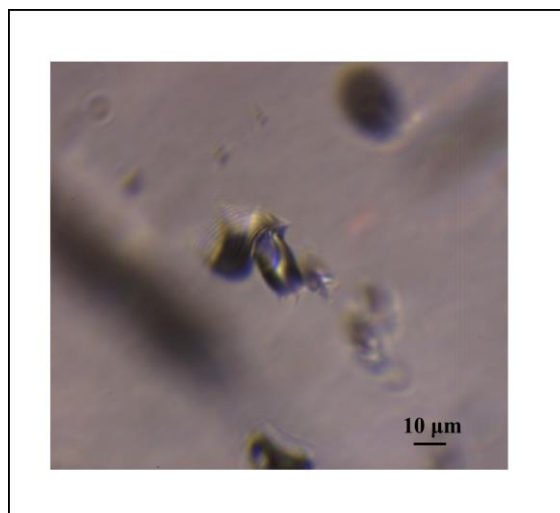


Figure 14. Two-phase (L + G) fluid inclusions.

I2: Tubular-shaped aqueous inclusion: this morphology would suggest a previous elongated fracture which was subsequently filled; the inclusion would therefore be secondary (S). Between 2900 and 3300 cm^{-1} we observe a large band of water; in this interval there are also three distinct large peaks at 2900 , 3200 and 3380 cm^{-1} and a weaker one diagnostic of water at 1630 cm^{-1} (Figure 15).

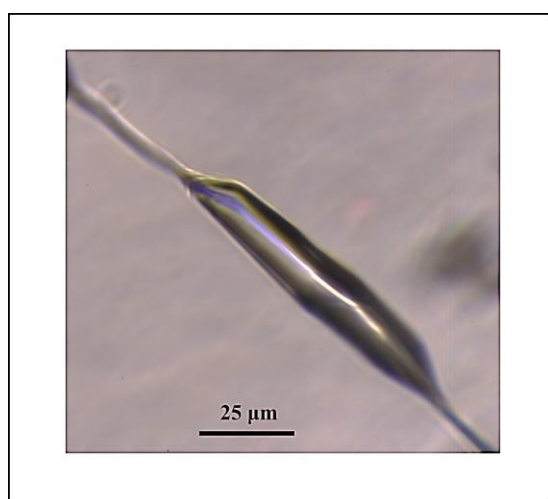


Figure 15. Tubular-shaped aqueous inclusion (L).

I3: Two-phase (L + G) hammer-shaped fluid inclusions: we can observe a large rounded bubble inside the inclusion and a smaller bubble above it. There are an absorption band at 2917 cm^{-1} related to CH_4 , an absorption peak at 2331 cm^{-1} typical of N_2 and a small band at 1555 cm^{-1} related to O_2 dissolved in water (Figure 16).

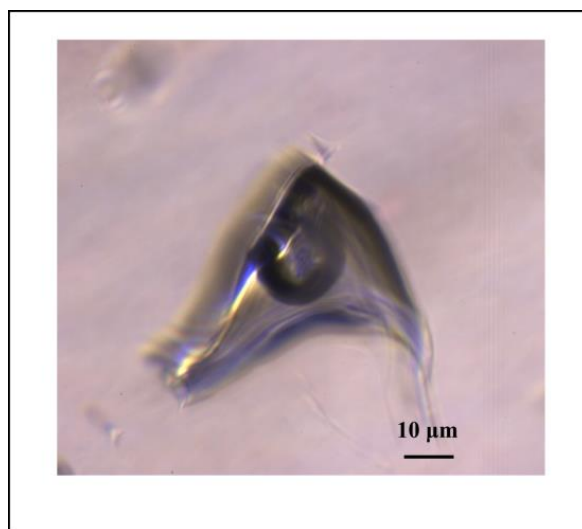


Figure 16. Two-phase (L + G) fluid inclusions.

I4: Polygonal two-phase (L + G) fluid inclusion: we observe the CH_4 band at 2900 cm^{-1} and N_2 at 2330 cm^{-1} (indicating a reducing environment), the water vapor band at 1550 cm^{-1} and two bands at 1370 and 1390 cm^{-1} which indicate the presence of CO_2 (Figure 17).

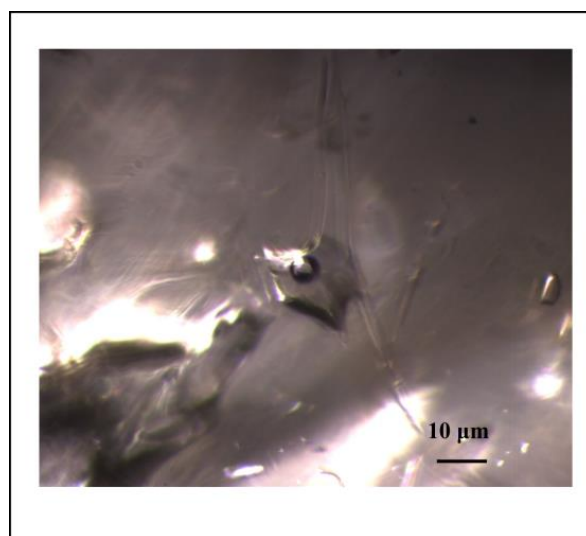


Figure 17. Polygonal two-phase (L + G) fluid inclusion surrounded by small oval inclusions.

Black inclusions: In sample 3, some black or dark inclusions were also analyzed, showing absorption bands at about 223 and 1313 cm^{-1} , which are characteristic of hematite. Under the gemological microscope, we observed the hematite appears as flakes within the datolite. There are also absorption bands at 104 and 138 cm^{-1} , due to fibrous and lamellar clinocllore inclusions.

5. Discussion and Conclusions

The investigations conducted in this work made it possible to evaluate the gemological properties of the Campotrera datolite for a possible use on the market. Datolite occurs into parent lithologies strongly altered by hydrothermal processes, but the mineral has not undergone the alteration and appears fresh. The most common form for this mineral is the double wedge, with a prism (110) and a pinacoid (001). Some of the investigated datolites are colorless or white creamy, while others are pinkish (salmon RGB color system) due to the presence of chromophore elements. We believe that Fe is the main chromophore

that gives Campotrera datolite its pink color; this element is present in varying amounts (36–1400 ppm) and is low or absent in creamy-white and colorless samples. However, we believe that our hypothesis could be further confirmed by spectroscopic analyses. Furthermore, even if the possibility of isomorphetic substitution cannot be excluded, we believe that Fe in colored datolites is mainly present in the inclusions of small crystals of hematite and ilmenite (see Raman graph in Appendix A). Hematite micro-inclusions are also the cause of chromatic inhomogeneities in the samples, which can also be observed with the naked eye.

Micro-Raman analysis showed the presence of different types of inclusions, in particular aqueous inclusions with gaseous methane (biphase L + G), aqueous (L) and methane inclusions. These different typologies would indicate that a part of the datolites was formed in a reducing environment in contact with fluids containing carbon.

The salinity values of the aqueous fluid inclusions are homogeneous (average 3.48) but differ from those in literature [3]. Regarding the genesis of these datolites, no definitive conclusions can be drawn from just the four inclusions studied. Additional studies of the cryothermometry of the various types of fluid inclusions with accurate determination of their homogenization temperatures and fluid properties are needed. The gems extracted from the raw sample are very appreciable: in addition to the beautiful color, they have high brilliance, transparency and birefringence, vitreous luster, no cleavage. The specific gravity and refractive index values are constant and well comparable with those in literature.

The gems extracted from the raw sample are very appreciable: in addition to the beautiful color, they have high brilliance, transparency and birefringence, vitreous luster, no cleavage. The specific gravity and refractive index values are constant and well comparable with those in literature.

Due to high birefringence, some of these gems show doubling of facet images when observed with the 10 × loupe. The cuts we have obtained are mixed or carré and the carat weight is between 1 and 5 carats which is a high value comparable to that of the datolite gems of the most renowned deposits.

The absence of cleavage allowed successful cutting operations; however, cutting requires extreme caution as the gems are only of medium hardness and occasionally exhibit fractures. To overcome these problems, we can use Campotrera datolites to create jewels to be worn occasionally, or the gems can be protected with structures such as bezels and prong settings. A bezel setting is essentially a metal band that wraps around the stone and is used primarily with the cabochon, while a prong setting consists of three or more metal prongs, or tines, that hold the gem in place and are used in faceted gems [10]. It is therefore possible to market this datolite not only as a collectible mineral but also as cut specimens for jewelry making.

In our previous work concerning black quartz from Val Secchia near Reggio Emilia, we highlighted how a correct exploitation of these minerals, carried out manually and in a sustainable way, can help create new jobs and therefore avoid the problem of abandonment of these mountain areas by young people [39]. In a similar way, datolites and other good-looking minerals from Campotrera could therefore favor the development of local craftsmanship for the production of jewelry and art objects, in a commercial context similar to that of “0 km food” a label indicating a type of food which is produced and sold locally. The difficulty of reaching outcrop sites has preserved these minerals from overexploitation and would increase their current value.

Author Contributions: Conceptualization, F.C. and M.S. methodology, L.M., F.C., M.G. and M.S.; validation, L.M., F.C., M.G. and M.S.; formal analysis, F.C. and M.G.; investigation, F.C. and M.G.; resources, L.M., F.C. and M.S.; data curation, L.M., F.C. and M.S.; writing—original draft preparation, L.M., F.C. and M.S.; writing—review and editing, L.M.; visualization, L.M.; supervision, L.M. All authors have read and agreed to the published version of the manuscript.

Funding: This research received no external funding.

Data Availability Statement: Not applicable.

Acknowledgments: We would like to sincerely thank Enrico Bonacina from Treviolo (BG) and Enrico Borghi (Società Reggiana di Scienze Naturali) for the photos on the gems; Omar Bartoli (Department of Geosciences, University of Padova) for the photo on the thin petrographic section; the Oriented Nature Reserve of Campotrera (RE) for allowing us to take some fragments of datolite.

Conflicts of Interest: The authors declare no conflict of interest.

Appendix A

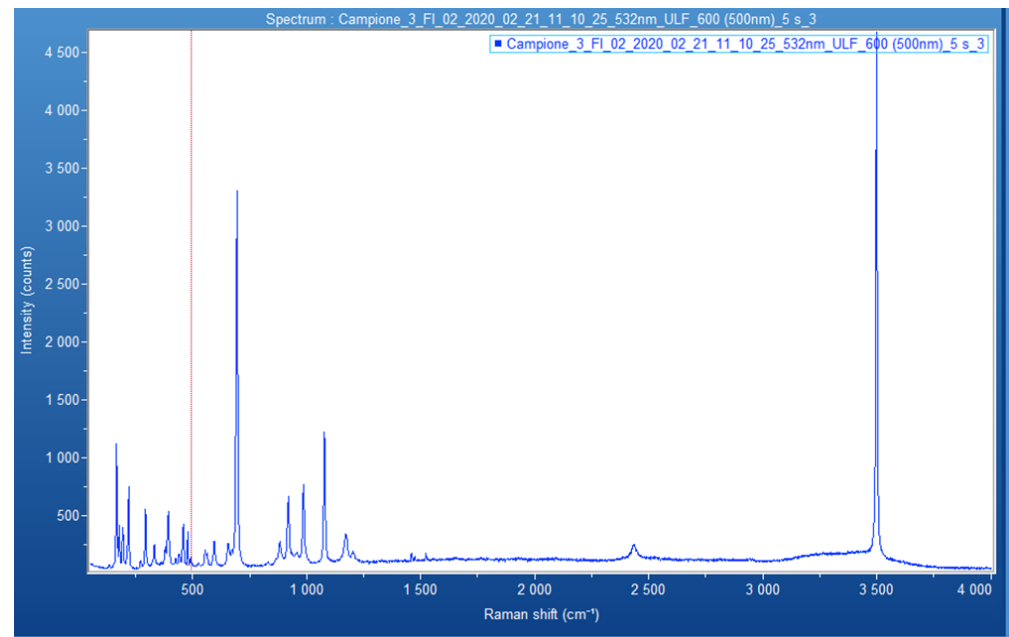


Figure A1. Raman Spectra of the primary aqueous inclusion (Figure 14).

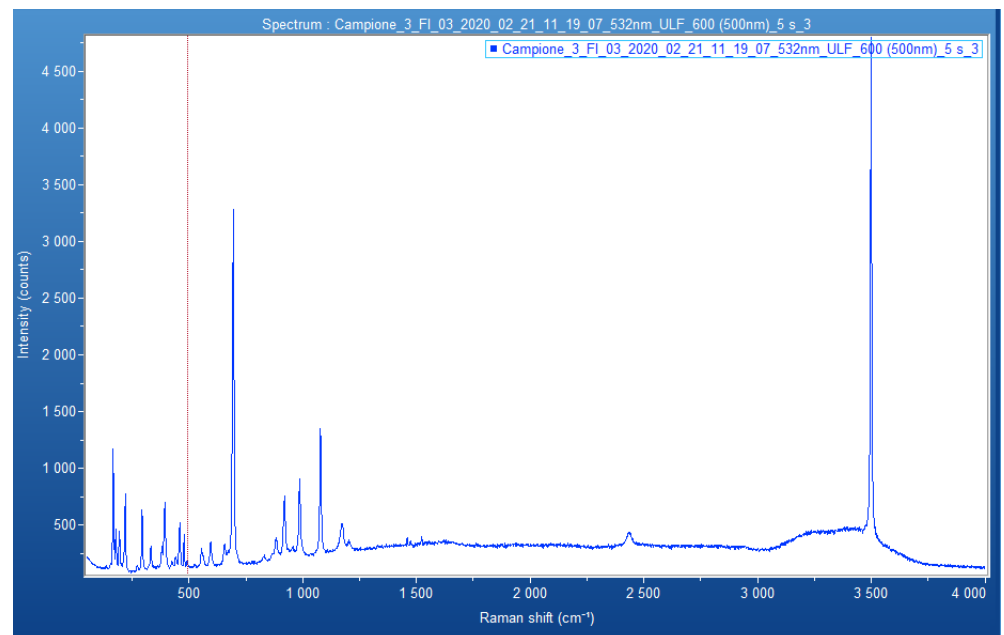


Figure A2. Raman spectra of the tubular-shaped aqueous inclusion (Figure 15).

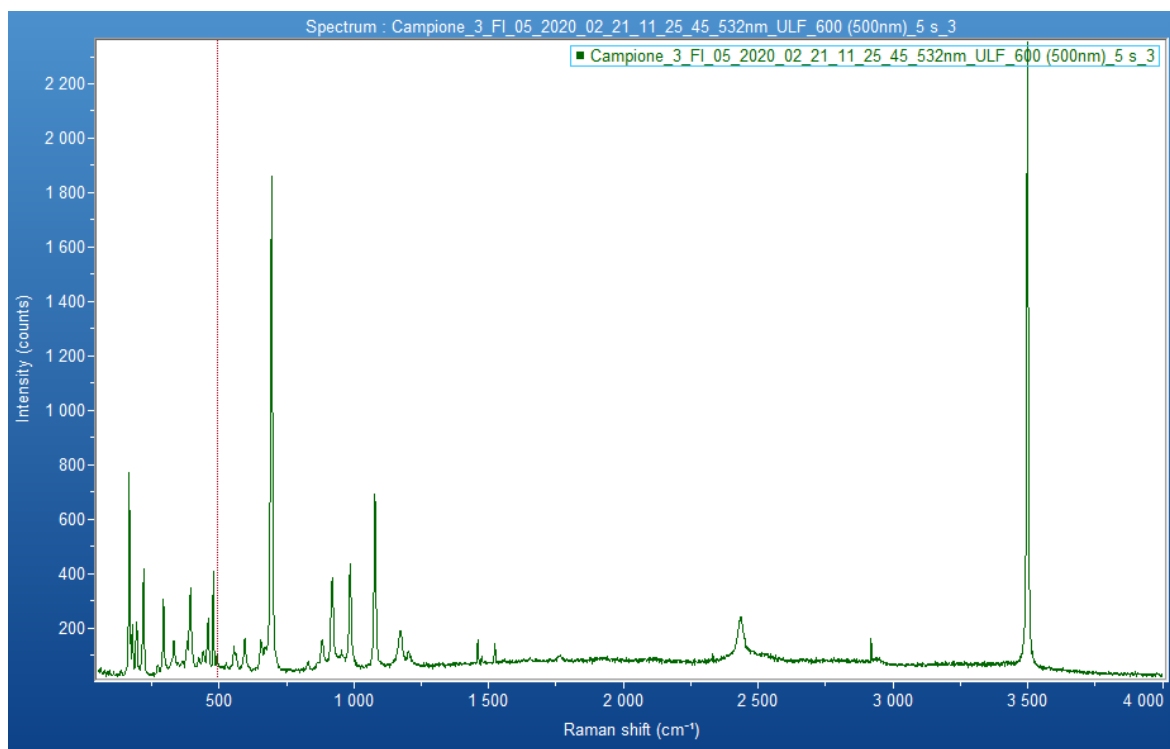


Figure A3. Raman spectra of the two-phase (L + G) hammer-shaped fluid inclusions (Figure 16).

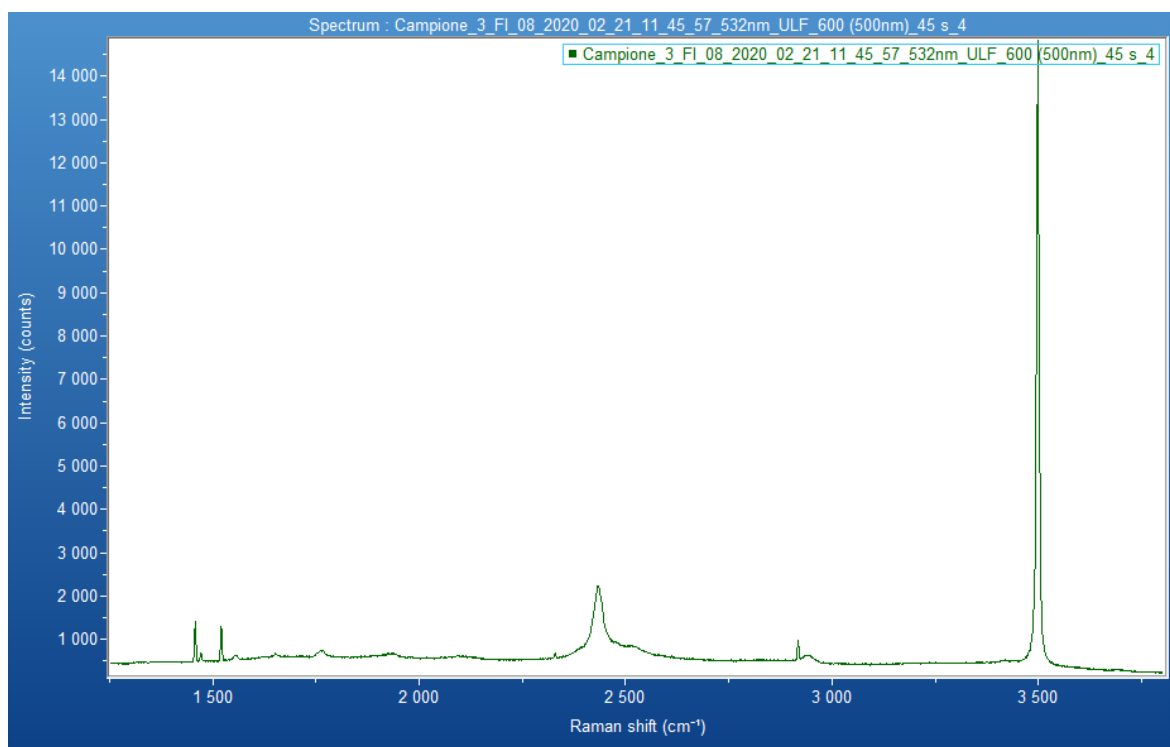


Figure A4. Raman spectra of the polygonal two-phase (L + G) fluid inclusion (Figure 17).

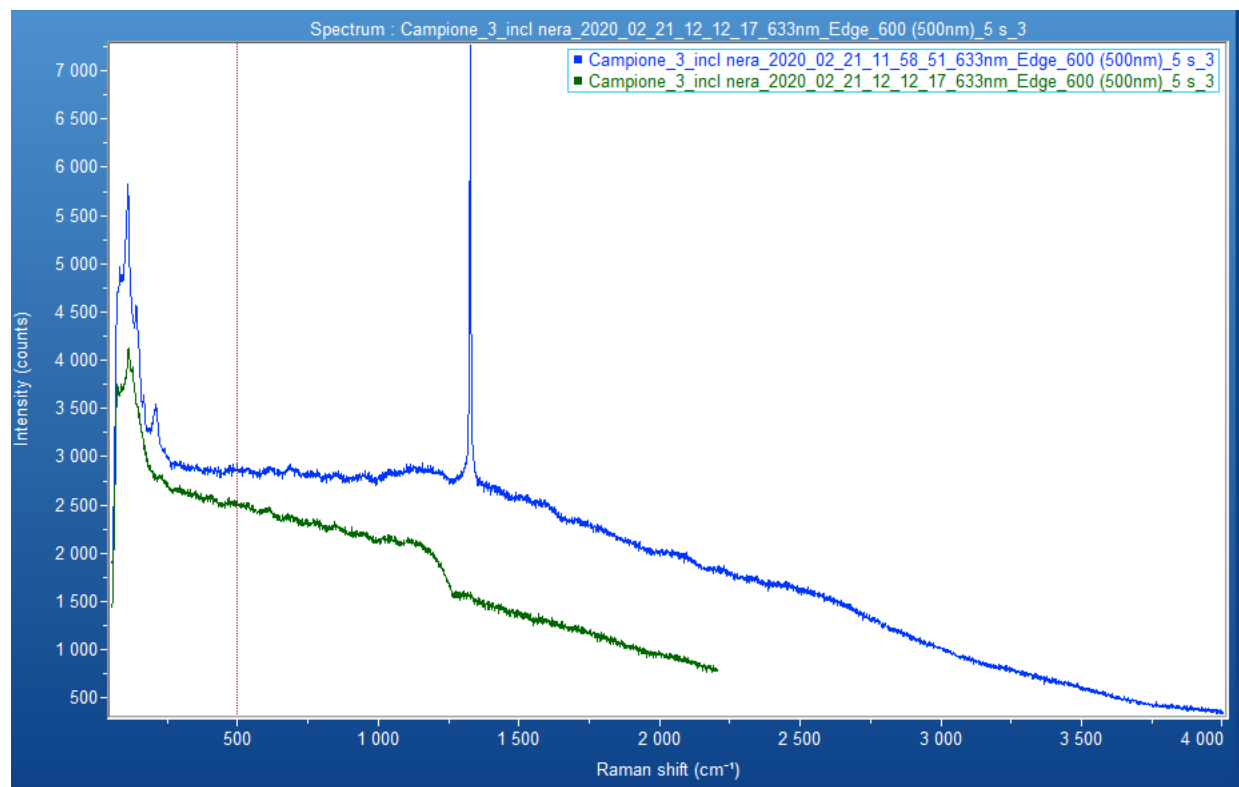


Figure A5. Raman spectra of the black inclusions.

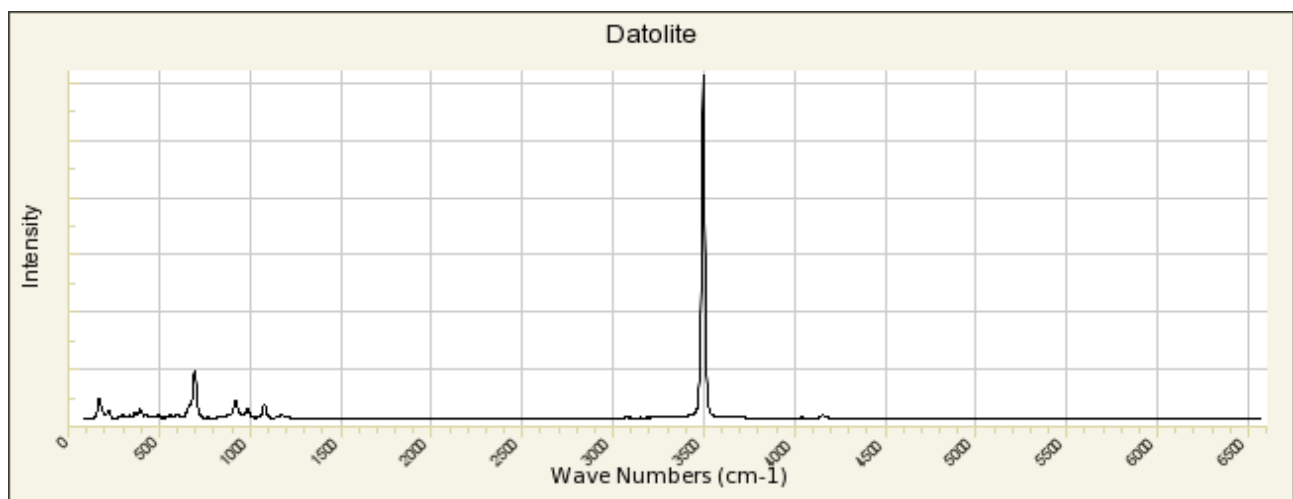


Figure A6. Raman spectra of datolite.

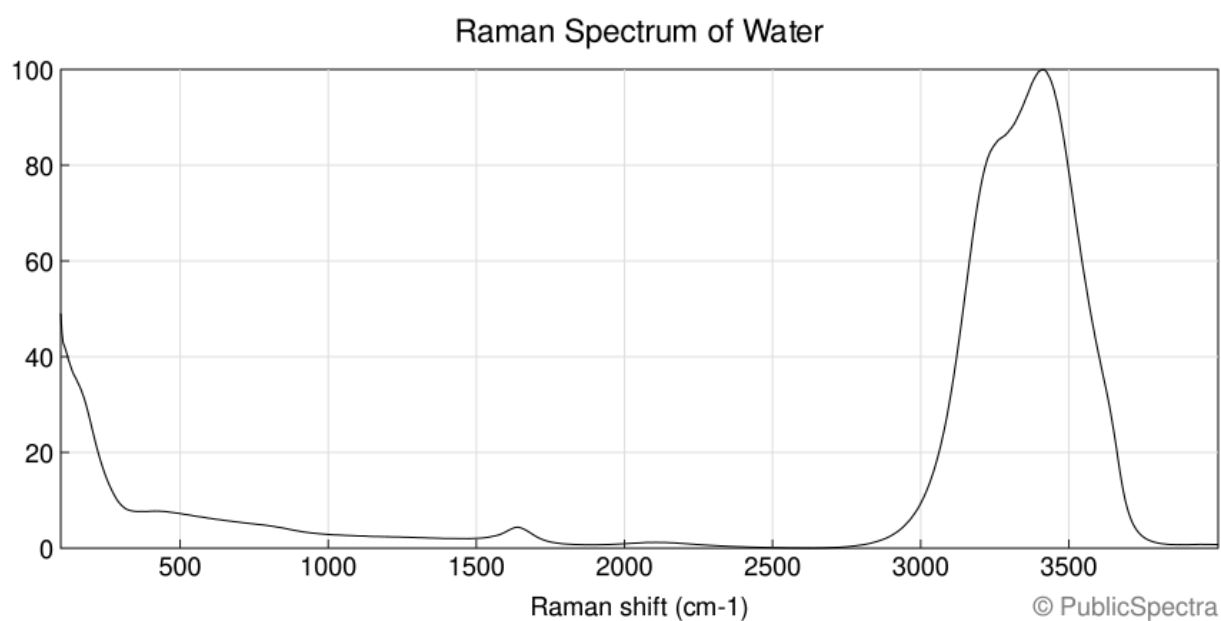


Figure A7. Raman spectra of water.

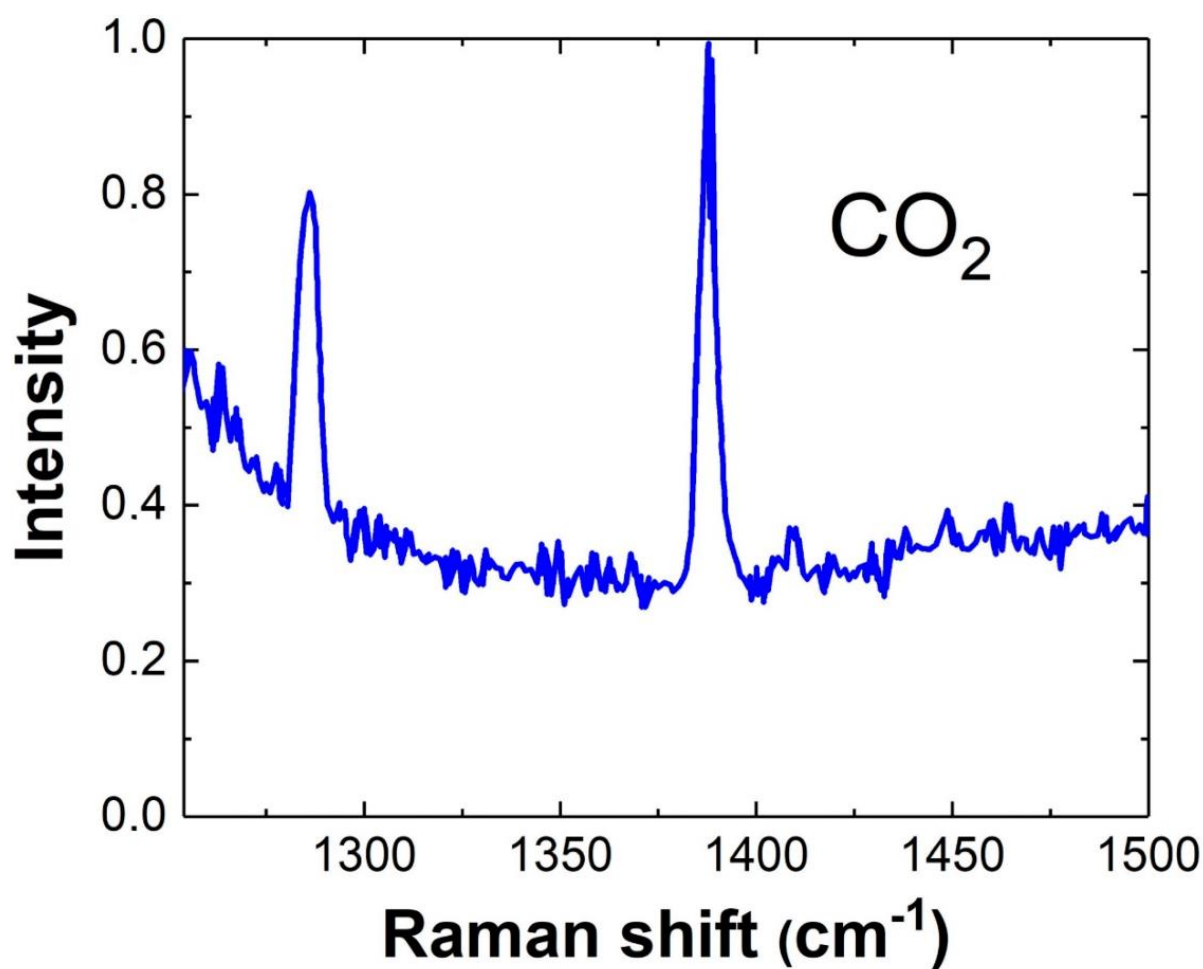


Figure A8. Raman spectra of CO₂.

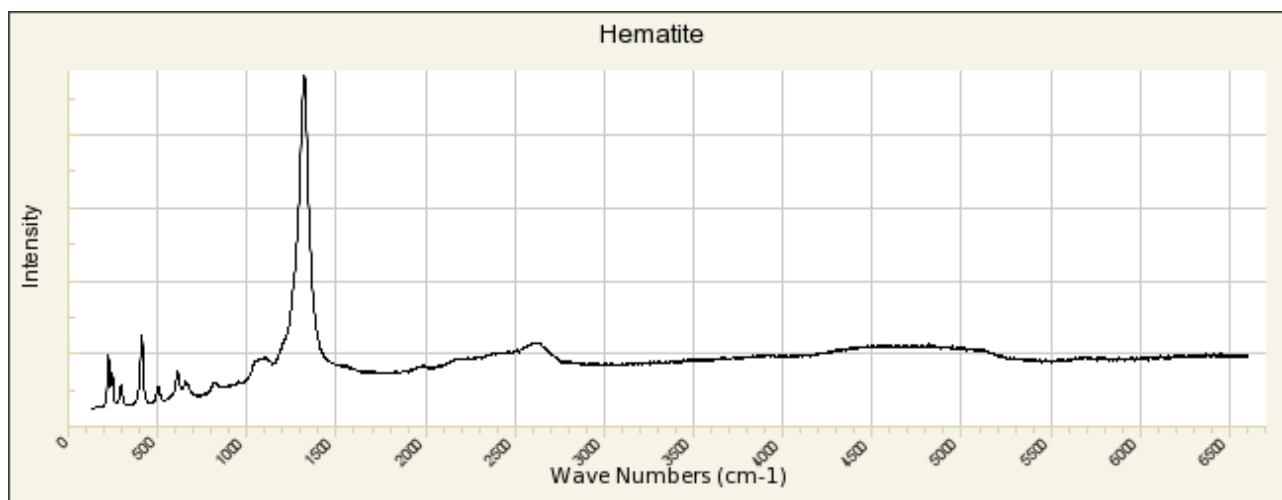


Figure A9. Raman spectra of hematite.

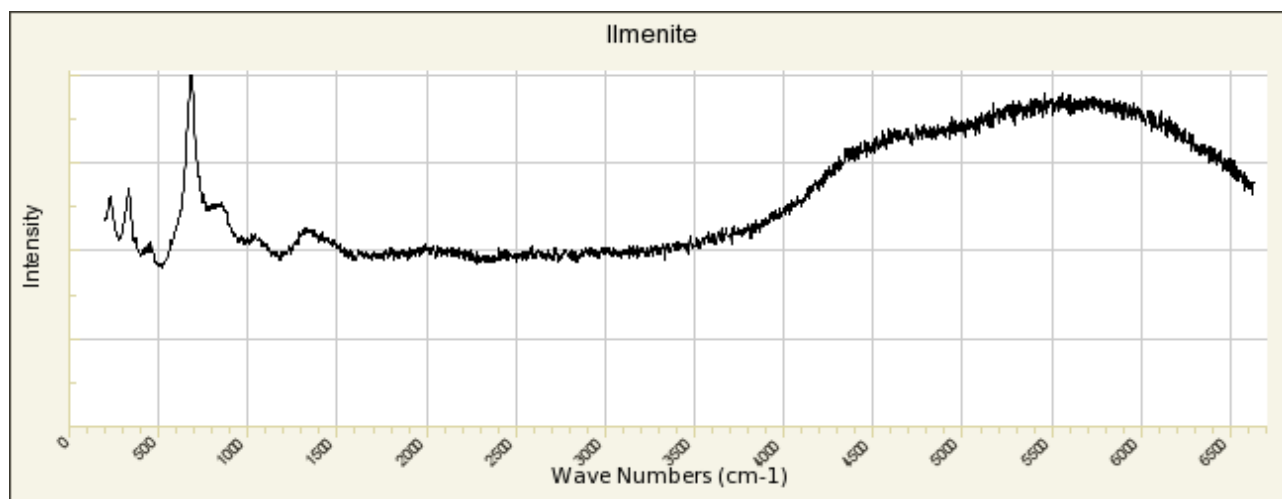


Figure A10. Raman spectra of ilmenite.

References

1. Borghi, E.; Scacchetti, M. L'attività estrattiva nella riserva naturale orientata Rupe di Campotrerà e nella zona di Rossena. *Comune Canossa* **2002**, *1*, 2–47.
2. Scacchetti, M.; Bartoli, O.; Bersani, D.; Laurora, A.; Lugli, S.; Malferrari, D.; Valeriani, L. Minerali della provincia di Reggio Emilia. *AMI Ed. Cremona* **2015**, 93–147.
3. Zaccarini, F.; Morales-Ruano, S.; Scacchetti, M.; Garuti, G.; Heide, K. Investigation of datolite ($\text{CaB}[\text{SiO}_4/\text{OH}]$) from basalts in the Northern Apennines ophiolites (Italy): Genetic implications. *Geochemistry* **2008**, *68*, 265–277. [\[CrossRef\]](#)
4. Foit, F.F.; Phillips, M.W.; Gibbs, G.V. A refinement of the crystal structure of datolite, $\text{CaBSiO}_4(\text{OH})$. *Am. Miner.* **1973**, *58*, 909–914.
5. Bellatreccia, F.; Camara, F.; Della Ventura, G.; Mottana, A. Datolite: A new occurrence in volcanic ejecta (Pitigliano, Toscana, Italy) and crystal-structure refinement. *Rend. Lincei* **2006**, *17*, 289–298. [\[CrossRef\]](#)
6. Bačík, P.; Fridrichová, J.; Uher, P.; Pršek, J.; Ondrejka, M. The crystal chemistry of gadolinite-datolite group silicates. *Can. Miner.* **2015**, *51*, 625–642. [\[CrossRef\]](#)
7. Bačík, P.; Miyawaki, R.; Fridrichová, J.; Atencio, D.; Cámara, F.; Fridrichová, J. Nomenclature of the gadolinite supergroup. *Eur. J. Miner.* **2017**, *29*, 1067–1082. [\[CrossRef\]](#)
8. Rinaldi, R.; Gatta, G.D.; Angel, R.J. Crystal chemistry and low-temperature behavior of datolite: A single-crystal X-ray diffraction study. *Am. Miner.* **2010**, *95*, 1413–1421. [\[CrossRef\]](#)
9. Perchiazzi, N.; Gualtieri, A.F.; Merlino, S.; Kampf, A.R. The atomic structure of bakerite and its relationship to datolite. *Am. Mineral.* **2004**, *89*, 767–776. [\[CrossRef\]](#)
10. Gemstones Encyclopedia. Available online: <https://www.gemsociety.org/> (accessed on 2 May 2023).
11. Datolite Gemstone Informations. Available online: <https://www.gemdat.org/> (accessed on 26 April 2023).

12. Konerskaya, L.P.; Orlova, R.G.; Bogdanis, E.P.; Konerskii, V.D.; Guseva, N.P. Using datolite and diopside raw materials in the electrical engineering industry. *Glass Ceram.* **1988**, *45*, 199–201. [\[CrossRef\]](#)
13. Medvedovski, E. Low-temperature sintering of ceramics for the production of low-voltage insulators. *Intern. Ceram. Rev.* **1996**, *45*, 82–86.
14. Bartoli, O.; Bersani, D.; Borghi, E.; Scacchetti, M. I minerali delle ofioliti: Rossena e Campotrera (RE). *Riv. Miner. It.* **2003**, *27*, 196–208.
15. Bartoli, O.; Bersani, D.; Borghi, E.; Garuti, G.; Morales-Ruano, S.; Scacchetti, M.; Zaccarini, F. Datolite di Valmozzola, Parma. Un ritrovamento eccezionale. *Riv. Miner. It.* **2008**, *32*, 8–15.
16. Kiss, G.; Molnar, F.; Zaccarini, F. Fluid inclusion studies in datolite of low grade metamorphic origin from a Jurassic pillow basalt series in northeastern Hungary. *Cent. Eur. J. Geosci.* **2012**, *4*, 261–274. [\[CrossRef\]](#)
17. Pezzotta, F.; Diella, V.; Guastoni, A. Chemical and paragenetic data on gadolinite-group minerals from Baveno and Cuasso al Monte, Southern Alps, Italy. *Am. Miner.* **1999**, *84*, 782–789. [\[CrossRef\]](#)
18. Ratkin, V.V.; Eliseeva, O.A.; Pandian, M.S.; Orekhov, A.A.; Mohapatra, M.; Priya, S.K.V. Stages and formation conditions of productive mineral associations of the Dalnegorsk borosilicate deposit, Sikhote Alin. *Geol. Ore Depos.* **2018**, *60*, 672–684. [\[CrossRef\]](#)
19. Datolite Mineral Information, Data and Localities. Available online: <https://www.mindat.org/> (accessed on 26 April 2023).
20. Boselli, F.; Boselli, L.; Ferretti, P.; Demartin, F. Datolite. Nuovo ritrovamento sul Buffaure (Val di Fassa, Trentino). *Riv. Miner. It.* **2013**, *2*, 108–115.
21. Albertini, C. Famous mineral localities: Baveno, Italy. *Miner. Rec.* **1983**, *14*, 157–168.
22. Marchesini, M.; Lunaccio, S.; Zampa, A. Il burrone di Vallegrande. *Riv. Miner. It.* **1988**, *4*, 19–24.
23. Riserva Naturale Rupe di Campotrera. Available online: <http://www.parchiemiliacentrale.it/riserva.rupe.campotrera/> (accessed on 1 March 2021).
24. Borghi, E.; Patteri, P.; Scacchetti, M. I minerali delle ofioliti di Campotrera e Rossena. *Comune Canossa* **2002**, 2–19.
25. Marroni, M.; Molli, G.; Montanini, A.; Tribuzio, R. The association of continental crust rocks with ophiolites in the Northern Apennines (Italy): Implications for the continent–ocean transition in the Western Tethys. *Tectonophysics* **1998**, *292*, 43–66. [\[CrossRef\]](#)
26. Marroni, M.; Molli, G.; Montanini, A.; Ottria, G.; Pandolfi, L.; Tribuzio, R. The external Liguride units (Northern Apennines, Italy): From rifting to convergence history of a fossil ocean-continent transition zone. *Ophioliti* **2002**, *27*, 119–132.
27. Montanini, A.; Tribuzio, R. Gabbro-derived Granulites from the Northern Apennines (Italy): Evidence for Lower-crustal Emplacement of Tholeiitic Liquids in Post-Variscan Times. *J. Petrol.* **2001**, *42*, 2259–2277. [\[CrossRef\]](#)
28. Montanini, A.; Tribuzio, R.; Vernia, L. Petrogenesis of basalts and gabbros from an ancient continent to ocean transition (External liguride ophiolites, Northern Italy). *Lithos* **2008**, *101*, 453–479. [\[CrossRef\]](#)
29. Tribuzio, R.; Thirlwall, M.F.; Vannucci, R. Origin of the gabbro-peridotite association from the Northern Apennine ophiolites (Italy). *J. Petrol.* **2004**, *45*, 1109–1124. [\[CrossRef\]](#)
30. Bertolani, M. La datolite della formazione ofiolitica appenninica. *Pontif. Accad. Sci.* **1948**, *12*, 305–366.
31. Ferrari, M. Sulla datolite del monte Campotrera. *Rend. R. Accad. Naz. Lincei* **1924**, *33*, 439.
32. Maddalena, L. Un nuovo giacimento di datolite e prehnite nell’Appennino Emiliano. *Period. Miner.* **1933**, *3*.
33. X-ray Diffractometers. Available online: <https://www.malvernpanalytical.com/> (accessed on 1 March 2021).
34. Miller, C.; Zanetti, A.; Thoni, M.; Konzett, J.; Klotzli, U. Mafic and silica-rich glasses in mantle xenoliths from Wau-ennamus, Lybia: Textural and geochemical evidence for peridotite melt reactions. *Lithos* **2012**, *128*, 11–26. [\[CrossRef\]](#)
35. Frezzotti, M.L.; Tecce, F.; Casagli, A. Raman spectroscopy for fluid inclusion analysis. *J. Geochem. Explor.* **2012**, *112*, 1–20. [\[CrossRef\]](#)
36. Roedder, E. Fluid Inclusions. In *Reviews in Mineralogy and Geochemistry*; Ribbe, P.H., Ed.; Mineralogical Society of America: Reston, VA, USA, 1984; Volume 12, p. 646.
37. Goldstein, R.H. Fluid inclusions in sedimentary and diagenetic systems. *Lithos* **2001**, *55*, 159–193. [\[CrossRef\]](#)
38. Caucia, F.; Scacchetti, M.; Marinoni, L.; Gilio, M. Black quartz from the Burano formation (Val Secchia, Italy): An unusual gem. *Minerals* **2022**, *12*, 1449. [\[CrossRef\]](#)
39. Mernagh, T.P.; Wilde, A.R. The use of the laser Raman microprobe for the determination of salinity in fluid inclusions. *Geochim. Cosmochim. Acta* **1989**, *53*, 765–771. [\[CrossRef\]](#)

Disclaimer/Publisher’s Note: The statements, opinions and data contained in all publications are solely those of the individual author(s) and contributor(s) and not of MDPI and/or the editor(s). MDPI and/or the editor(s) disclaim responsibility for any injury to people or property resulting from any ideas, methods, instructions or products referred to in the content.